[Mapping 3D multiples to CIGs]Imaging and mapping 3D multiples to image gathers: Example with a Gulf of Mexico dataset

SUMMARY

In this chapter, I migrate a real 3D seismic dataset from the Gulf of Mexico with shot profile migration. The dataset contains specular water-bottom multiples, peg-leg multiples associated with a large, shallow salt body, and diffracted multiples originating at the salt edges. Both the water bottom and the salt body have significant cross-line dip which makes it difficult to model the trajectory of the multiples and to apply 3D SRME. The location of the multiples in the image domain is severely affected by the presence of the salt and thus do not follow the geometry of the multiple-generating interface. As a consequence, some multiples could easily be interpreted as primaries. I show that primaries and multiples (even subsalt) can be discriminated by their different moveouts in SODCIGs and ADCIGs as in Chapter **??**.

INTRODUCTION

The Gulf of Mexico dataset, provided by VeritasDGC, was acquired over a complex salt body with structure in both the inline and the cross-line directions. The water-bottom dips in some places as much as 11 degrees in the cross-line direction making the mapping of the multiples in the image-space cube difficult to predict. The presence of the salt distorts the multiples so much that in many cases it is difficult to discern with any certainty which events are multiples and which events are primaries in the migrated cube. An important tool for that purpose are the SODCIGs where the multiples can be identified by their tendency to map away from zero inline and crossline subsurface offsets, and the ADCIGs where primaries should be flat as a function of aperture angle while multiples exhibit residual moveout as I showed in Chapter **??**.

I first migrate a sail line, with shot profile migration, to assess the possibility of discriminating between primaries and multiples on inline subsurface offsets, where, according to the results of Chapter **??**, there is better chance of imaging the multiples. The results are encouraging and show in several places that enough differential curvature exists between primaries and multiples in inline SODCIGS and ADCIGs even below salt. The image cube, however, is poor because of the large crossline dips that require that much more than one sail line be migrated in order to capture the flanks of the salt bodies and in one case even its top and bottom. The multiples, of course, are also improperly migrated in just one sail line. I then migrate the entire dataset with a large crossline migration aperture. Due to computer limitations, only a relatively small inline migration aperture was used and no prestack image gathers were created. The image cube shows great improvement in the image of the salt flanks as well as the top and bottom salt reflections that were missing from the migration of

only one sail line. The steepest salt flanks are still poorly imaged because of the limitations in the amount of available data. This image cube was used to select a smaller dataset below a small salt body, to perform a full-fledged shot profile migration with the computation of prestack images in both the inline and crossline directions.

In this chapter I will compare the different prestack image domains and show the behavior of the primaries and multiples, in particular subsalt multiples. I will defer until the next chapter the actual attenuation of the multiples.

DESCRIPTION OF THE DATA

Acquisition geometry

The 3D dataset consists of 20 sail lines each with four active streamers and dual flip-flop shooting. The separation between streamers is 160 m and between receivers is 25 m. The shot interval is 37.5 m (between the flip and the flop). The minimum offset inline is 240 m and each streamer has 288 receivers for a maximum inline offset of 7175 m. Figure 1 shows the acquisition template. Figure 2 shows a map view of the subset of the shots used in this thesis. Although most sail lines were straight in the East-West direction, a few had significant curvature.

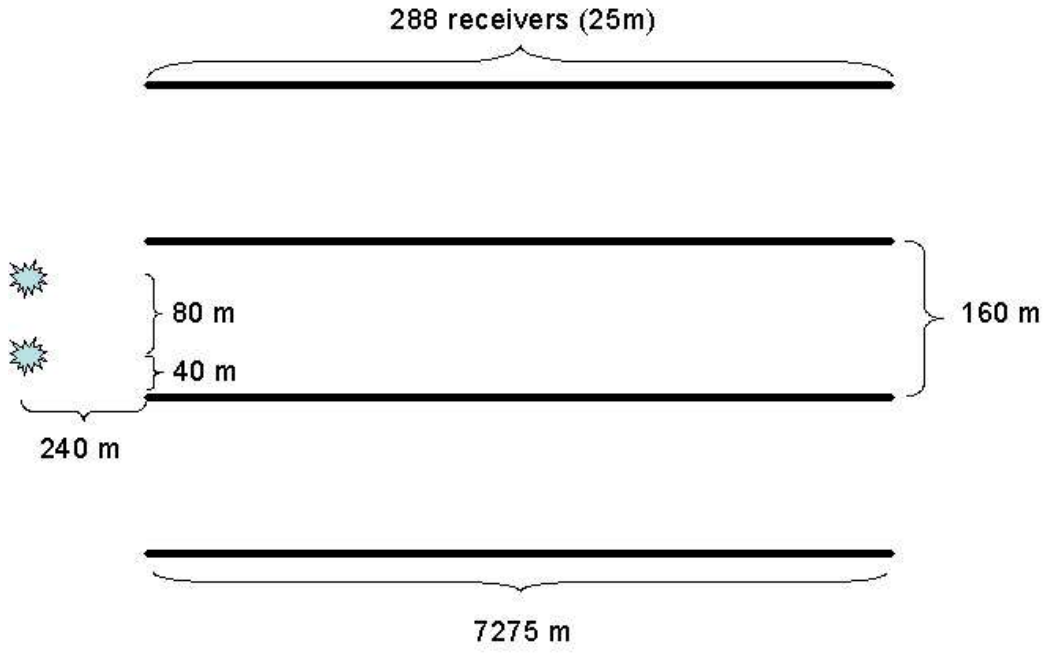

Figure 1: Sketch of the basic acquisition geometry

The strong currents present in the area caused significant feathering. Figure 3 shows an example for the sail-line at cross-line distance 11440 m (see Figure 2. The feathering angle is about 25 deg with respect to the inline direction. For most shots,

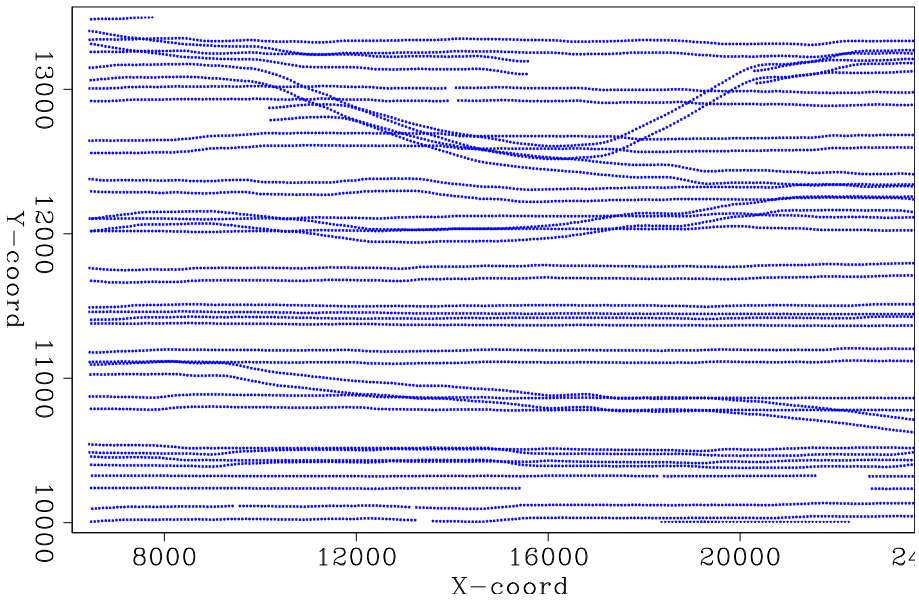

Figure 2: Map view of the source locations.

the feathering was in the same South-North direction. Figure 4 shows the fold of coverage that in some places depart significantly from its design value of 48. Some of the short source lines in Figure 2 were acquired as infill to avoid large coverage holes.

Migration velocity model

The migration velocity model (provided by Norsk Hydro), shows a large, complex salt body with steeply dipping flanks in both inline and cross-line directions (Figure 5). The water-bottom itself dips in some places as much as 11 degrees in the cross-line direction, although it is relatively flat in the inline direction.

SHOT PROFILE MIGRATION

Attempting to migrate and compute 3D angle gathers for the entire dataset would be way too expensive, so I started by migrating the data without computing prestack 3D images. The idea is to obtain a good image that can be used to select a smaller, subsalt dataset, on which to compute the image gathers. Table 1 shows the parameters and data extent used for this migration.

In order to efficiently migrate the data with shot profile migration, I removed the time samples before the water-bottom arrival. This is equivalent to time-shifting the data (changing its origin) and I compensated for it by applying a linear frequency shift to the source wavelet. The propagation through the water layer was done in two depth steps and from there down the depth sampling was 10 m. The propagation

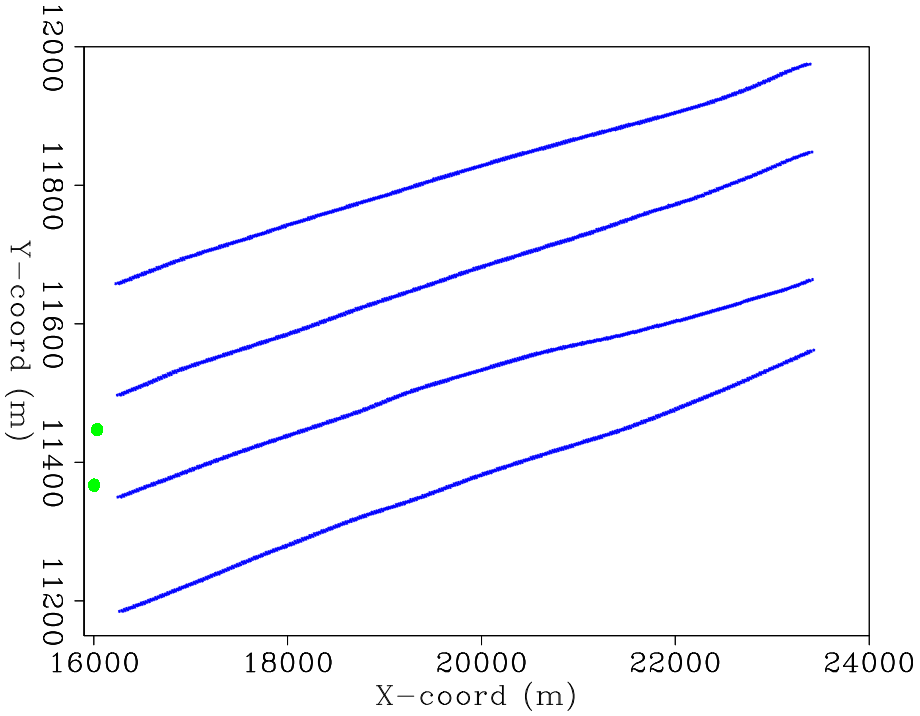

Figure 3: Map view of the receiver cables for one shot illustrating typical feathering. The feathering angle is about 25 deg with respect to the inline direction.

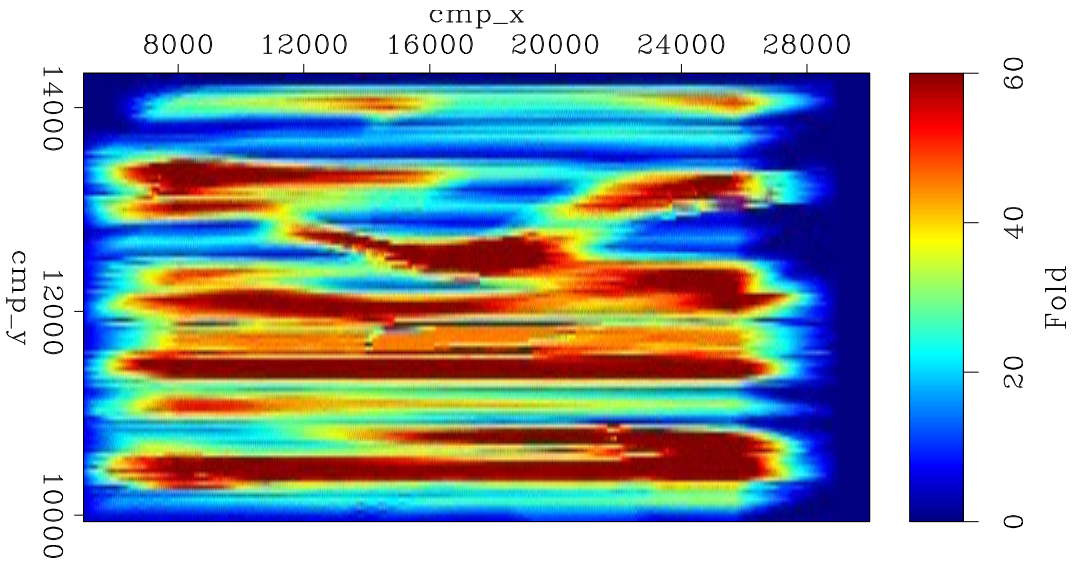

Figure 4: Fold map illustrating relatively uniform coverage.

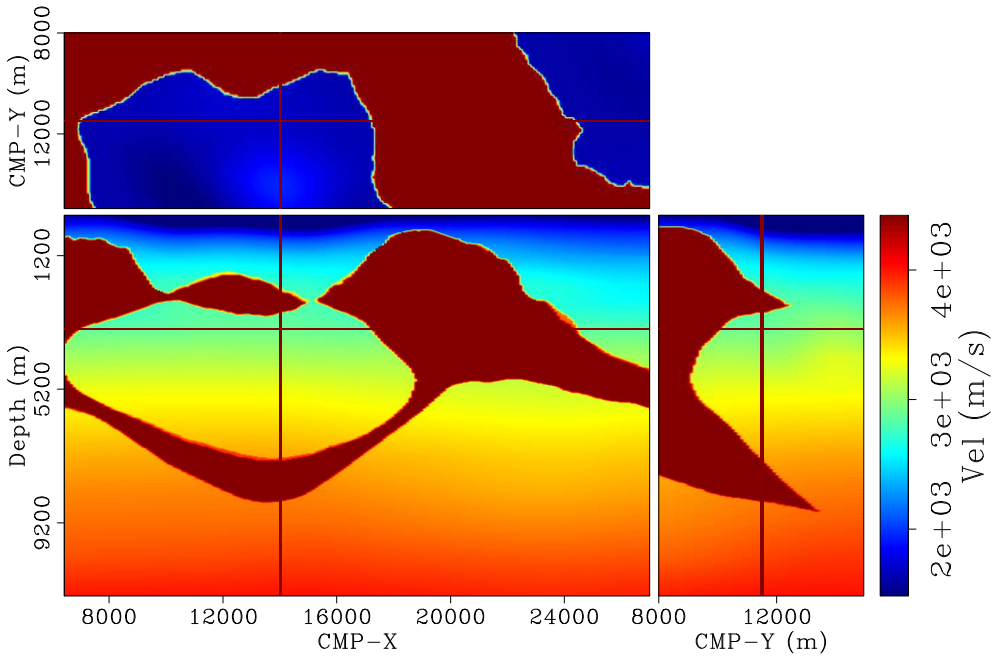

Figure 5: Subsurface velocity model. Note the strong dips in both the inline and cross-line directions.

Table 1: Migration parameters and data extent for full migration.

Inline			Crossline		
Min CMP	Max CMP	Aperture (m)	Min CMP	Max CMP	Aperture (m)
5000	32000	10000	10000	14000	4000

was done with a Phase Shift Plus Interpolation algorithm (**??**). For the sake of computer time, only two reference velocities, computed with Lloyd's algorithm (**?**), were used to propagate the data at each depth step. Four hundred frequencies were used from 6 to 40 Hz. A total of 8600 shots were migrated. Figure 6 shows an inline section taken at CMP-Y=11840 m. Again, recall that the depth axis is with respect to an arbitrary reference. The migrated data was filtered in depth and a gain proportional to the depth squared was applied for display purposes. Both the top and bottom reflections of the smaller salt body are well imaged, as are most subsalt reflections directly below it. The salt bottom reflection for the larger salt body is also well imaged but its right flank is poorly imaged because of lack of data. The available dataset did not extend enough beyond CMP-X=25000 m to capture the corresponding reflections. Notice what seems to be a multiple below 4000 m depth, specially around CMP-X=16000 m. The rectangle encloses the subset image that was deemed most promising to illustrate the attenuation of subsalt multiples. A new shot profile migration, including the computation of prestack images was carried out on this subset of the data.

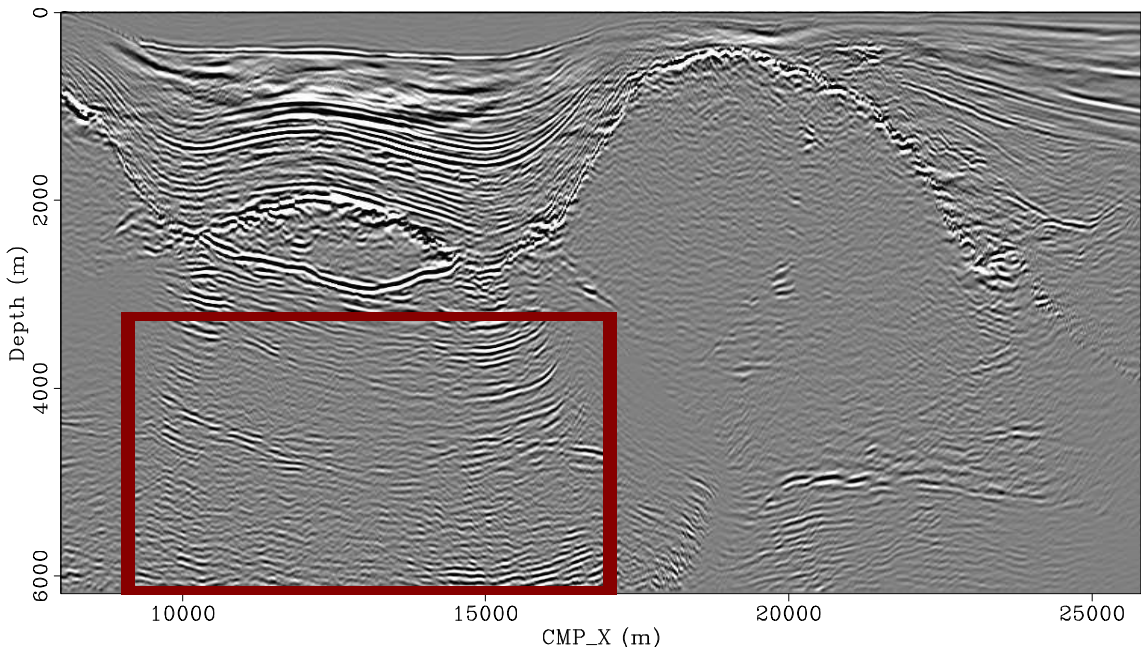

Figure 6: Shot profile migration. Inline image section at crossline CMP 11440 m. The rectangle encloses the subset of the image for which a new migration was performed including the computation of prestack images.

Figure 7 shows the crossline image section taken at CMP-X=12000 m. Notice that the bottom of the salt and the subsalt reflections deteriorate to the left of about CMP-Y=11500 m. This again is due to lack of available data to the left of CMP-Y=10000 m. Here again the rectangle encloses the subset of the data to attempt the attenuation of subsalt multiples.

PRESTACK MIGRATED IMAGES

Based on the results of the previous section, I computed the full-fledged shot profile migration of the selected sub-salt dataset, including the computation of three-dimensional image gathers. The migration parameters and the range of data migrated are summarized in table 2. Four reference velocities were used at each depth extrapolation step, chosen with Lloyd's algorithm. Two hundred and fifty frequencies were used in the range 6-38 Hz. Three hundred depth extrapolation steps were taken at 10 m depth interval. A total of 4300 shots were migrated.

The result of the shot profile migration is a five-dimensional cube that is challenging to visualize. I will show some of the more common prestack subsets of the data to give an idea of the mapping of both primaries and multiples in the migrated domain. Figure 8 shows the 3D image cube taken at zero inline and zero crossline subsurface offsets. The top panel shows a depth slice at 4630 m where there is a hint of a multiple cutting through the primary reflections shown in the inline section (left

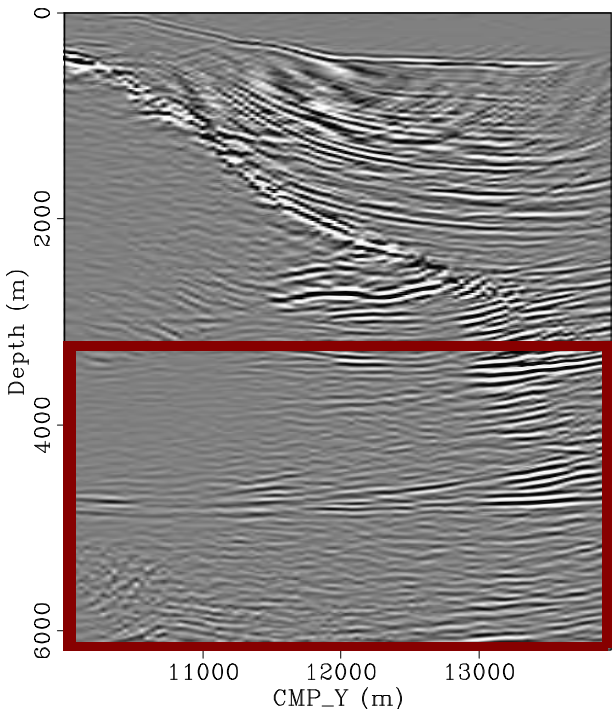

Figure 7: Shot profile migration. Crossline image section at inline 12000 m. The rectangle encloses the subset of the image for which a new migration was performed including the computation of prestack images.

Table 2: Migration parameters and data extent. The minimum and maximum offsets refer to the subsurface offsets for the SODCIGs.

Inline				
Min CMP	Max CMP	Min OFF (m)	Max OFF (m)	Aperture (m)
9000	17000	-750	250	8000
Crossline				
Min CMP	Max CMP	Min OFF (m)	Max OFF (m)	Aperture (m)
10000	14000	-600	600	4000

panel) and pointed to by the arrow. This inline section is taken at CMP-Y=13000 m. The right panel shows the crossline section at CMP-X=14400 m. It is very difficult to discriminate which of these subsalt reflections are primaries and which are multiples without the help of prestack migrated images. The image in the crossline direction (right panel) is not nearly as clear because of the relatively few crossline CMPs that went into the prestack migration. This makes the identification of multiples in that panel even more difficult.

Ideally, the primaries should migrate to zero inline and zero crossline subsurface offsets. Errors in migration velocity and illumination problems may make them shift away from zero subsurface offsets, but in most situations these shifts away from zero subsurface offset are minor when compared to those of the multiples for which the difference between propagation and migration velocity is large. Therefore, we can expect that the primaries and the multiples be relatively easy to identify by their

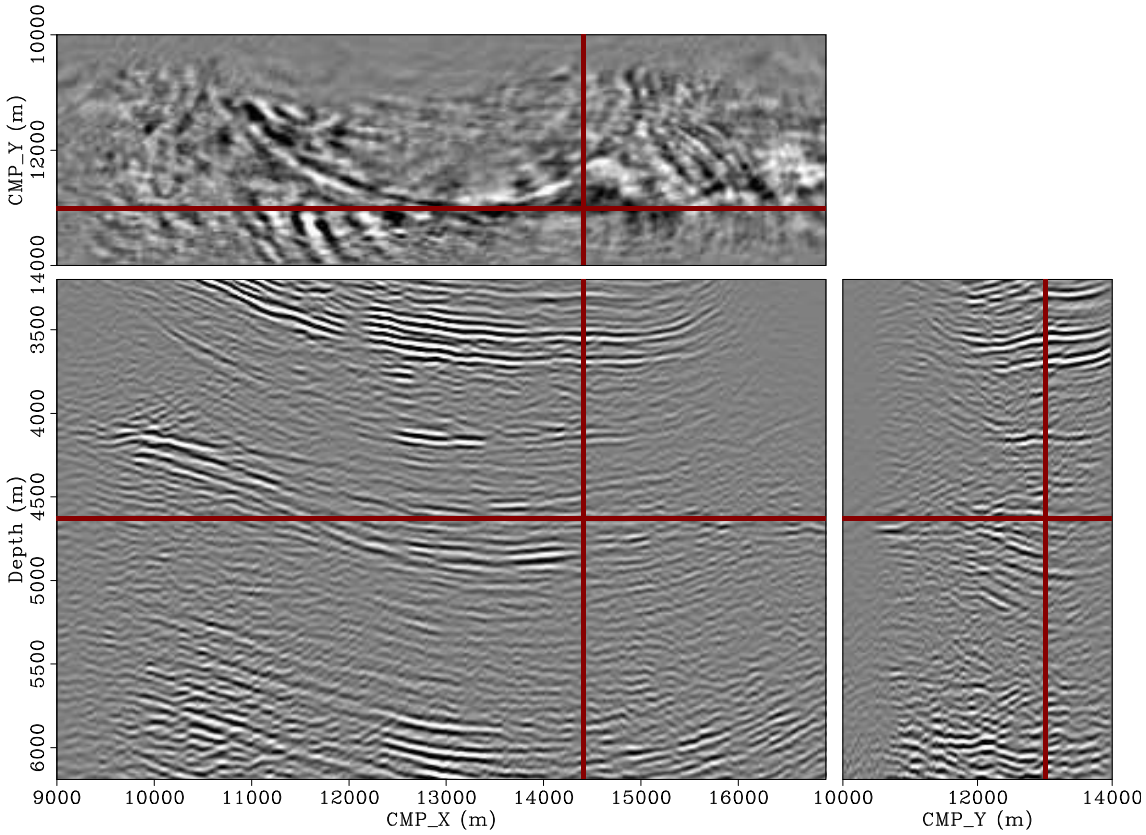

Figure 8: Shot profile migration. Zero subsurface offset cube. Top panel is a depth slice at 6430 m, left panel is the inline section at crossline 13000 m and right panel is the crossline section at inline 14400 m.

mapping in both the inline and crossline subsurface offsets. Figure 9 shows one 3D SODCIG taken at the spatial location CMP-X=14400 m and CMP-Y=13000 m (see Figure 8). The inline offset gather (panel (a)), corresponds to OFF-Y=0 while the crossline offset gather (panel (b)), corresponds to OFF-X=-500 m. In the inline offset gather we see that the primaries map near zero offset (above 3000 m) whereas the multiples map entirely to the negative subsurface offsets (around 4500 m and below 5500 m). Since the crossline offset gather is taken at the inline offset of the multiple (-500 m), the primaries are absent and the multiples map to both positive and negative subsurface offsets. This is a consequence of the geometry of acquisition that had positive inline surface offsets only but positive and negative crossline surface offsets. Notice also that more subsurface offsets, specially in the crossline direction, should have been computed in order to capture the multiples in their entirety.

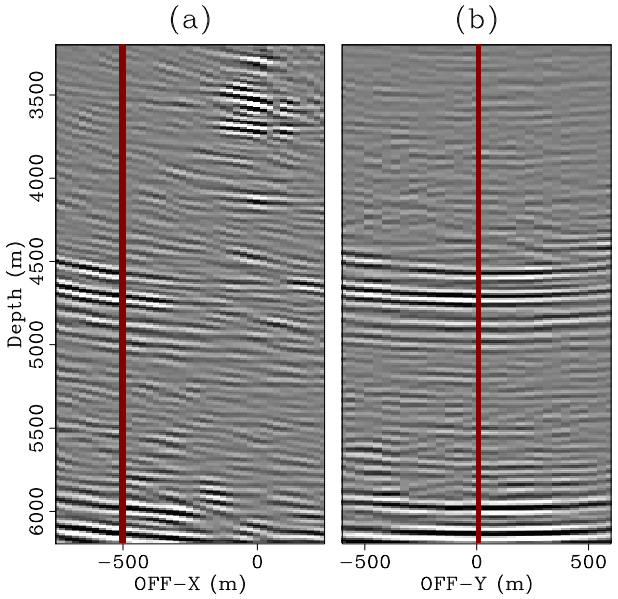

Figure 9: Shot profile migration. SODCIG at CMP-X=14400 m and CMP-Y=13000 m. Panel (a) is the inline offset gather taken at OFF-Y=0 and panel (b) is the crossline offset gather taken at OFF-X=-500 m.

Figure 10 shows a subset of the five dimensional hyper-cube taken at CMP-Y=13000 m and OFF-Y=0 m. There is, therefore, no crossline information on this figure. Panels (a) and (c) show the inline sections at zero and -400 m inline subsurface offsets respectively, while the middle panel shows the inline gather at CMP-X=14400. Since the crossline offset is zero in all the panels, we can expect to see the primaries near the zero inline offset in panel (b) and as the dominant reflections in panel (a). The multiples (at least those that did not map away from zero crossline offset), we can expect to find at the negative inline offsets in panel (b) and as the dominant reflections in panel (c). Notice how it would have been very hard to visually distinguish primaries and multiples without the aid of these prestack images.

To take an even closer look at the multiples, Figure 11 shows a similar figure to Figure 10 but for CMP-X=9900 m. This time both panels (a) and (c) correspond mostly to multiples. An interesting observation is that the residual moveout of the multiple in panel (b) seems to have its bottom away from zero inline subsurface offset, indicating perhaps a diffracted multiple. Furthermore, recall that this inline plane is

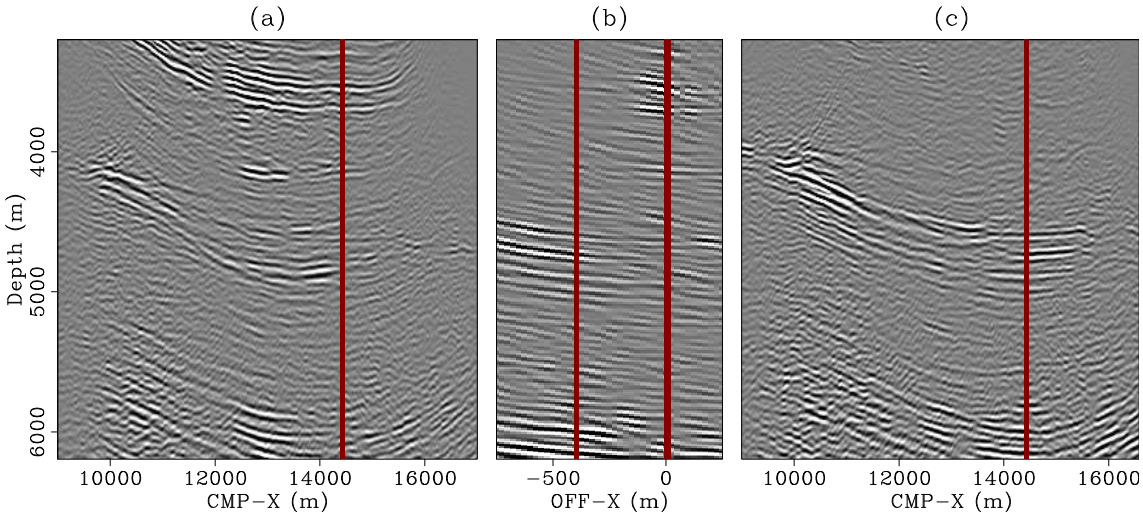

Figure 10: Inline section and inline offsets at CMP-Y=13000 m and OFF-Y=0. Panel (a) is the inline section at zero inline offset. Panel (b) is the inline offsets at CMP-X=14400 m and Panel (c) is the inline section at -400 m inline offsets. Panel (a) should be mostly primaries while panel (c) should be mostly multiples.

taken at zero crossline offset. The situation is even more manifest if the section is taken at a crossline offset away from zero.

Finally, to illustrate the mapping of the multiples in the crossline direction, Figure 13 shows the subset taken at CMP-X=14000 m and OFF-X=0. As with the previous two figures, panel (a) corresponds to the crossline section at OFF-Y=0 while panel (c) is a similar section at OFF-Y=-400 m. The middle panel corresponds to the crossline offset gather. Here also the primaries should map to panel (a) while some of the multiples (those that did not map away from zero inline offset), should map to panel (c). In panel (b) we can see that the primaries map near zero crossline offset while the multiples map away from zero both to positive and negative subsurface offsets. Similarly, Figure 14 shows the subset taken at the same CMP-X location but at OFF-X=-600 m. Both panels (a) and (c) should now correspond to multiples and no primaries should be mapped to any of these panels.

MULTIPLES IN ADCIGS

I will now show the results of computing the 3D angle gathers from the SODCIGs shown in the previous section. Figure 15 shows two 3D angle gathers. The first one (panel (a)) is taken at CMPX=14000 m and CMPY=13500 m and the second one (panel (b)) at CMPX=11000 m and CMPY=13000 m. The 3D ADCIG in Panel (a) shows two strong primaries at the top and and weak multiples at the bottom. Notice in the depth slice a pattern similar to the one obtained for the synthetic data primary in Chapter **??** (recall panel panel (a) of Figure **??**). Notice also that the azimuth

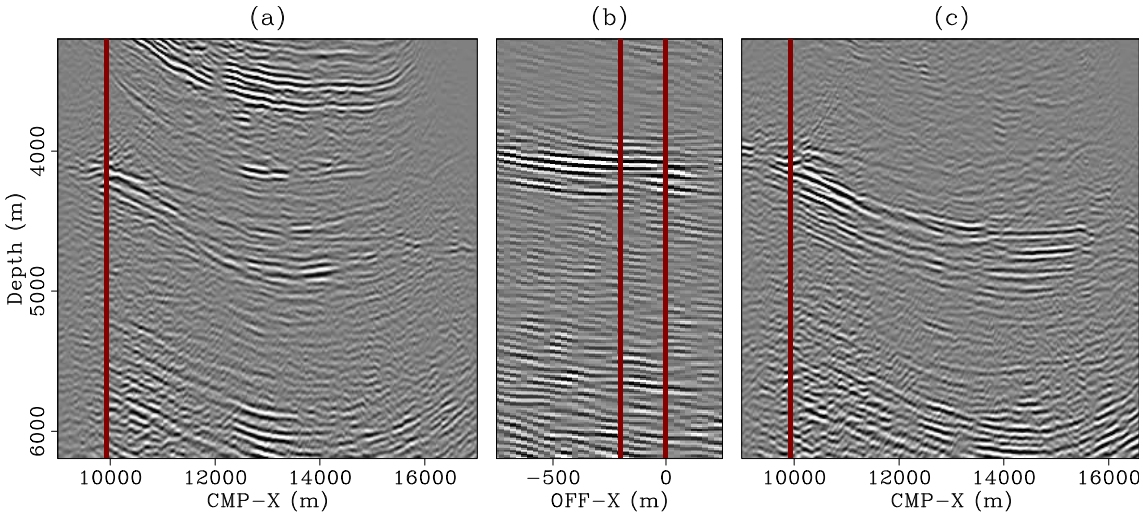

Figure 11: Inline section and inline-offset gather at CMP-Y=13000 m and OFF-Y=0. Panel (a) is the inline section at zero inline offset. Panel (b) is the inline offsets at CMP-X=9900 and Panel (c) is the inline section at -200 m inline offsets. Panel (a) is mostly primaries and panel (c) is mostly multiples.

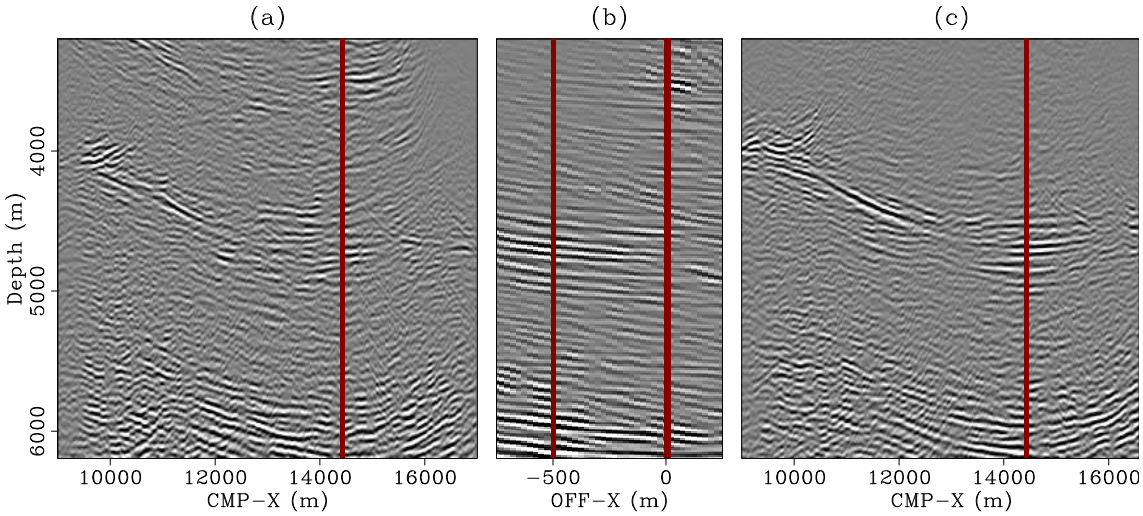

Figure 12: Inline section and inline-offset gather at CMP-Y=13000 m and OFF-Y=-400. Panel (a) is the inline section at zero inline offset. Panel (b) is the inline offsets at CMP-X=14400 and Panel (c) is the inline section at -500 m inline offsets. Panel (a) has some contributions from primaries and multiples whereas panel (c) should be almost exclusively multiples.

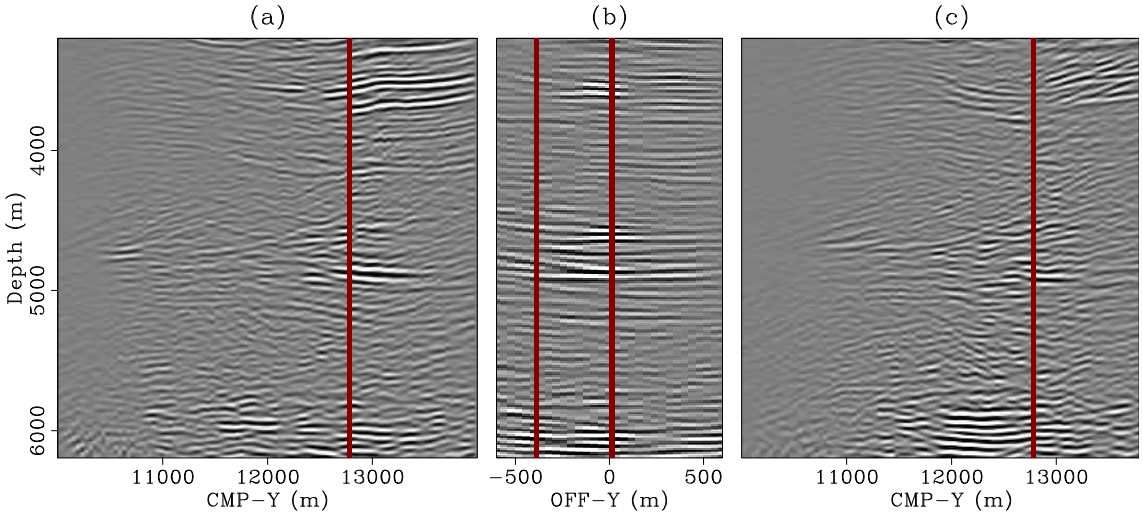

Figure 13: Shot profile migration. Crossline section and crossline offsets at CMP-X=14000 m and OFF-X=0. Panel (a) is the crossline section at zero crossline offset. Panel (b) is the crossline offsets at CMP-Y=12760 m and Panel (c) is the crossline section at -400 m crossline offsets. Panel (a) should be mostly primaries while panel (c) should be mostly multiples.

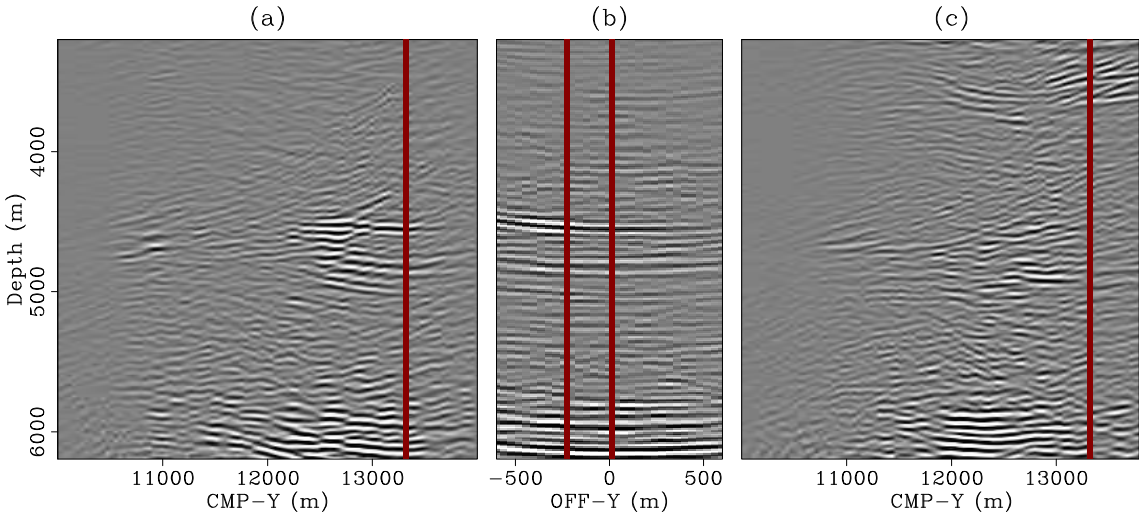

Figure 14: Shot profile migration. Crossline section and crossline offsets at CMP-Y=14000 m and OFF-X=-600. Panel (a) is the crossline section at zero crossline offset. Panel (b) is the crossline offsets at CMP-Y=13300 m and Panel (c) is the crossline section at -240 m crossline offsets. Both panels (a) and panel (c) should be multiples.

coverage of the primaries decreases (that is, the azimuth resolution increases), as the aperture angle increases. The two primaries focus at slightly different azimuths as seen in the azimuth gather of panel (a). The 3D ADCIG in Panel (b), on the other hand, shows a weak primary at the very top and a strong multiple at the bottom. Again, the depth slice is consistent with the one obtained for the synthetic data multiple in Chapter **??** (recall panel (b) of Figure **??**) and, contrary to the primary, shows a broad range of azimuth coverage at large aperture angles.

In order to investigate the variation of the residual moveout of primaries and multiples with reflection azimuth, I plot in Figure 16 the angle gather at location CMPX=13000 m and CMPY=13000 m for aperture angles of 0, 5, 10, 15 and 20 degrees. At zero aperture angle (panel (a)), neither the primaries nor the multiples show any azimuth resolution. As the aperture angle increases, the primaries are focused to a relatively narrow range of azimuths (panel (e) above 5500 m) whereas the multiples are essentially scattered. Similarly, Figure 17 shows the same gathers but at location CMPX=14000 m and CMPY=14000 m. Again, notice the azimuth focusing of the weak primaries at the top (panel (e)) and the upswings of the multiple (panels (c), (d) and (e)). The lack of azimuth focusing of the multiples with increasing aperture angle is a consequence of the crossline dip and velocity lateral velocity variations that cause the multiple path to be very complex with no defined azimuth even for large aperture angle.

Finally, to investigate the variation of the residual moveout of the primaries and the multiples with aperture angle, Figures 18 and 17 show angle gathers at reflection azimuths of -40, -20, 0, 20, 40 at the same locations as Figures 16 and 19, respectively. Notice that in both figures the moveout of the primaries is flat at all the azimuths that illuminate the reflector whereas the multiple shows the expected over-migrated moveout. It is interesting to see that the multiple essentially disappears in panel (e) of Figure 18 indicating that it was not illuminated at that azimuth (at least not in the aperture range of 0 to 20 degrees). This is somewhat in contrast to the results for the synthetic data in Chapter **??** that indicated that the multiple was illuminated with an azimuth range similar to that of the primary (compare the depth slices in panels (a) and (b) of Figure **??**. This is not the case with this real data (compare the depth slices in panels (a) and (b) of Figure 15) for which the multiples seem to be illuminated preferentially at small aperture angles. A similar behavior is well known with 2D data.

DISCUSSION

The results of Chapter **??** indicated that we could discriminate between primaries and multiples in inline subsurface offset gathers but perhaps not in the crossline subsurface offset. In this chapter I showed that we can discriminate between primaries and multiples in both subsurface offset directions if there is enough crossline dip.

A full 3D migration with large inline and crossline migration apertures is necessary

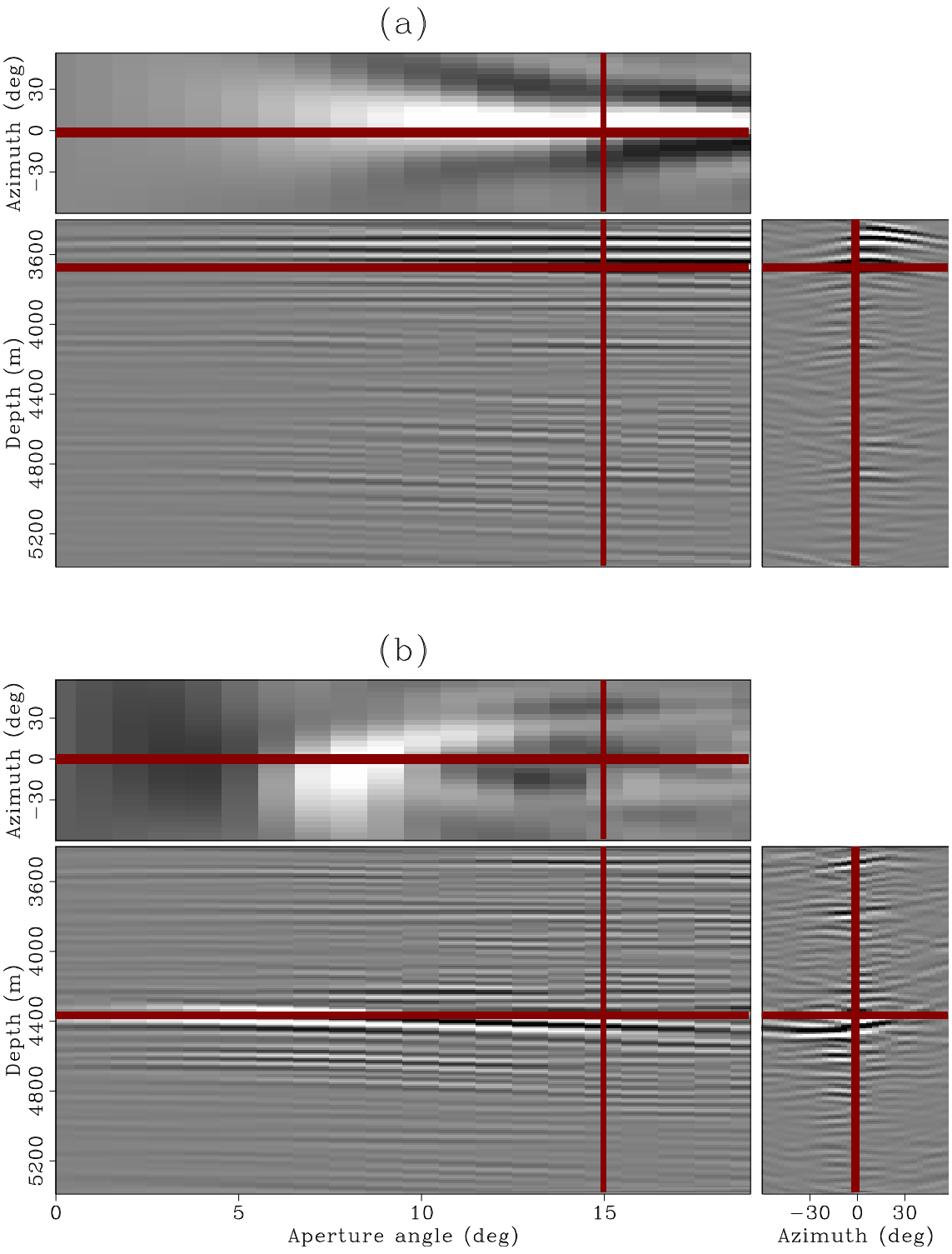

Figure 15: 3D angle gathers. (a) at CMPX=14000 m and CMPY=13500 m. (b) at CMPX=11000 m and CMPY=13000 m. Notice the strong primaries above 5500 m depth in panel (a) and the strong multiple below 6000 m depth in panel (b).

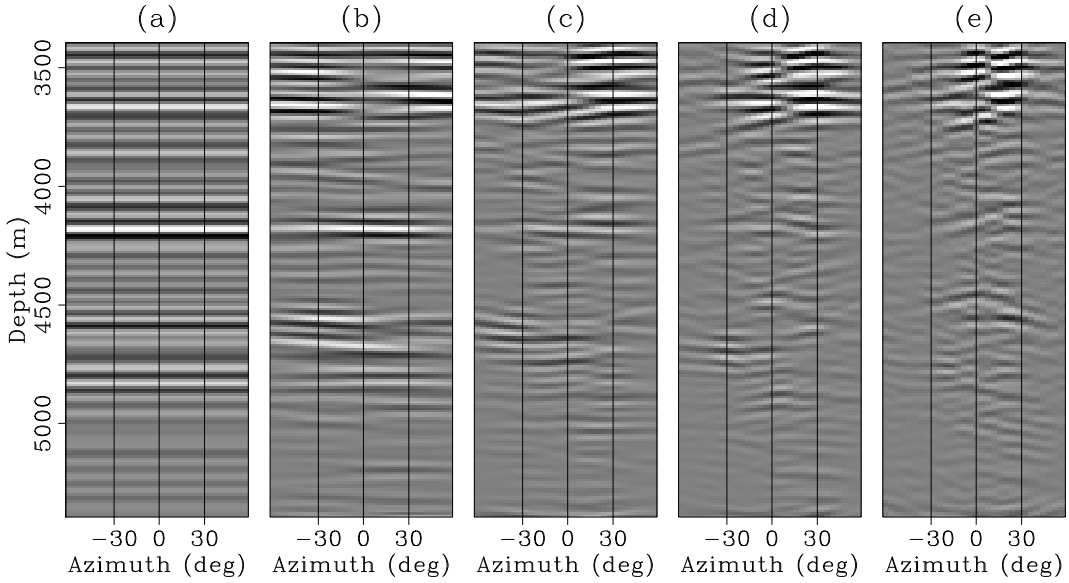

Figure 16: 3D angle gathers as a function of azimuth for aperture angles of 0, 5, 10, 15 and 20 degrees (panels (a) through (e)). The gather is taken at CMPX=13000 m and CMPY=13000 m.

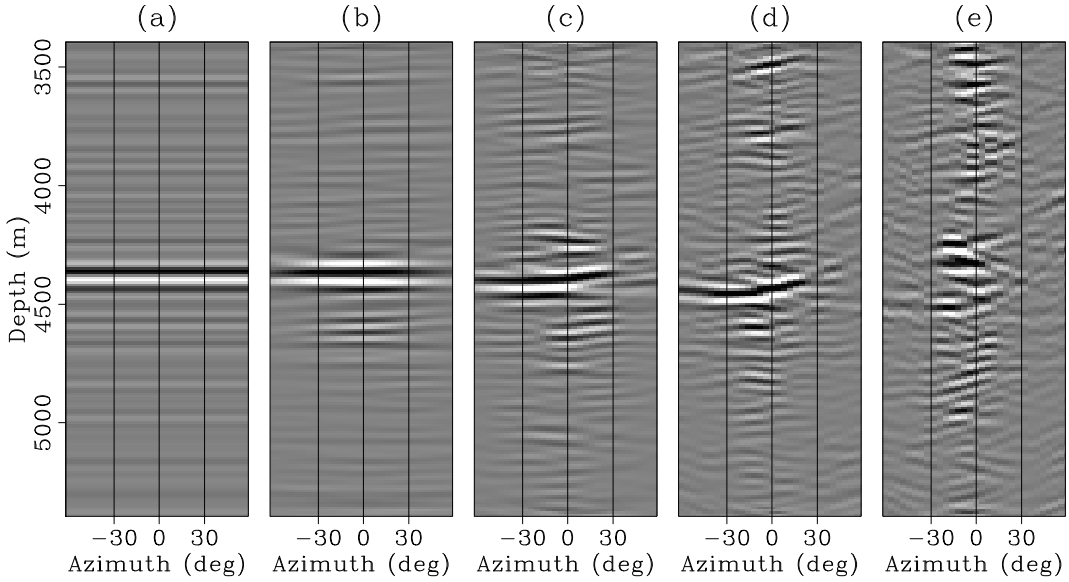

Figure 17: 3D angle gathers as a function of azimuth for aperture angles of 0, 5, 10, 15 and 20 degrees (panels (a) through (e)). The gather is taken at CMPX=11000 m and CMPY=13000 m.

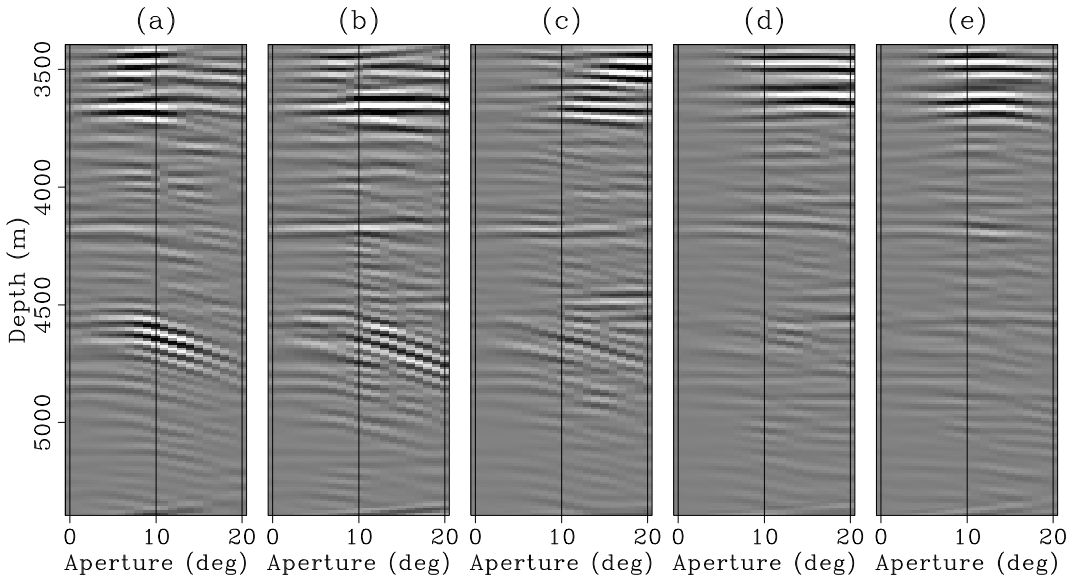

Figure 18: 3D angle gathers as a function of aperture angle for reflection azimuths of -40, -20, 0, 20 and 40 degrees (panels (a) through (e)). The gather is taken at CMPX=13000 m and CMPY=13000 m.

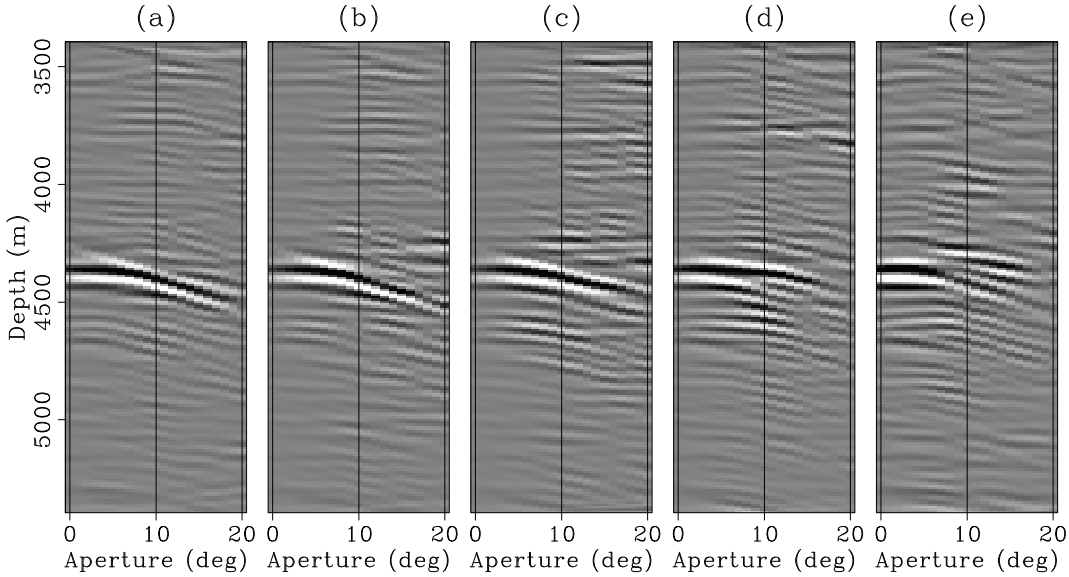

Figure 19: 3D angle gathers as a function of aperture angle for reflection azimuths of -40, -20, 0, 20 and 40 degrees (panels (a) through (e)). The gather is taken at CMPX=11000 m and CMPY=13000 m.

to correctly image the multiples. To attenuate the multiples we need to compute prestack image gathers as a function of subsurface offset or aperture and azimuth angles. Below salt both primaries and multiples are illuminated only by a narrow range of aperture angles. This makes the difference in moveout between primaries and multiples relatively small. In fact, if we consider only inline subsurface offset gathers at zero crossline subsurface offset and vice-versa, the difference in moveout may indeed be too small. But we need to remember that in a way that is the worst case scenario because the difference between the moveout of primaries and multiples in inline subsurface offsets is larger at non-zero crossline subsurface offsets and vice-versa. Similarly for the 3D ADCIGs.

It is challenging to fully appreciate all the information in the five-dimensional SODCIGs or ADCIGs and just looking at individual planes gives only glimpses of the true difference between the primaries and the multiples. The main message of this chapter is that we can indeed discriminate between them even for subsalt reflections. In the next chapter I go into the craft of actually attenuating the multiples in the Radon domain.

CONCLUSIONS

Complex subsurface distorts multiples and make their identification difficult in the image space. SODCIGs help in discriminating between primaries and multiples but are expensive to compute. 3D ADCIGs are even more expensive to compute but can be used to attenuate the multiples as will be shown in the next chapter.

ACKNOWLEDGMENTS

I would like to thank CGGVeritas for providing the dataset and Dr. Jan Pajchel of Norsk Hydro for providing the velocity model and for his help in securing permission to use the dataset.